

Constraining the Flavor Structure of Lorentz Violation Hamiltonian with the Measurement of Astrophysical Neutrino Flavor Compositions

Kwang-Chang Lai,^{1,*} Wei-Hao Lai,^{2,†} and Guey-Lin Lin^{2,‡}

¹*Center for General Education, Chang Gung University, Kwei-Shan, Taoyuan, 333, Taiwan*

²*Institute of Physics, National Chiao Tung University, Hsinchu, 300, Taiwan*

We study Lorentz violation effects to flavor transitions of high energy astrophysical neutrinos. It is shown that the appearance of Lorentz violating Hamiltonian can drastically change the flavor transition probabilities of astrophysical neutrinos. Predictions of Lorentz violation effects to flavor compositions of astrophysical neutrinos arriving on Earth are compared with IceCube flavor composition measurement which analyzes astrophysical neutrino events in the energy range between 25 TeV and 2.8 PeV. Such a comparison indicates that the future IceCube-Gen2 will be able to place stringent constraints on Lorentz violating Hamiltonian in the neutrino sector. We work out these expected constraints for different flavor structures of Lorentz violating Hamiltonian. In some cases these expected constraints can improve upon the current constraints obtained from other types of experiments by more than two orders of magnitudes.

PACS numbers: 95.85.Ry, 14.60.Pq, 95.55.Vj

* kcl@mail.cgu.edu.tw

† s9927525.py99g@g2.nctu.edu.tw

‡ glin@mail.nctu.edu.tw

I. INTRODUCTION

Although physical laws are believed to be invariant under Lorentz transformation, violations of Lorentz symmetry might arise in string theory as discussed in [1, 2]. It is possible to incorporate Lorentz violation (LV) effects in an observer-independent effective field theory, the so-called Standard-Model Extension (SME) [3, 4], which encompasses all the features of standard model particle physics and general relativity plus all possible LV operators [5–7]. While LV signatures are suppressed by the ratio $\Lambda_{\text{EW}}/m_{\text{P}}$ with Λ_{EW} the electroweak energy scale and m_{P} the Planck scale, experimental techniques have been developed for probing such signatures [8, 9]. The effects of LV on neutrino oscillations were pointed out in [10–12]. One can categorize LV effects to neutrino flavor transitions into three aspects: the modifications to energy dependencies of neutrino oscillation probabilities, the directional dependencies of oscillation probabilities, and the modifications to neutrino mixing angles and phases. In the standard vacuum oscillations of neutrinos, the oscillatory behavior of flavor transition probability is determined by the dimensionless variable $\Delta m^2 L/E$ with Δm^2 the neutrino mass-squared difference, L the neutrino propagation distance, and E the neutrino energy. This dependence results from the Hamiltonian $H_{\text{SM}} = UM^2U^\dagger/2E$ with $M_{ij}^2 = \delta_{ij}(m_j^2 - m_1^2)$. The extra terms in Lorentz violating Hamiltonian H_{LV} introduces L and LE dependencies into the oscillation probability, in addition to the standard L/E dependence. The directional dependence of oscillation probability is due to the violation of rotation symmetry in H_{LV} . The coefficients of LV operators change periodically as the Earth rotates daily about its axis. This induces temporal variations of neutrino oscillation probability at multiples of sidereal frequency $\omega_\oplus \approx 2\pi/(23 \text{ h } 56 \text{ min})$. Finally the full Hamiltonian $H \equiv H_{\text{SM}} + H_{\text{LV}}$ is diagonalized by the unitary matrix V which differs from U due to the appearance of H_{LV} . Hence the values of neutrino mixing angles and phases associated with V deviate from those associated with U . Such deviations increase with neutrino energies since H_{SM} is $\mathcal{O}(E^{-1})$ while H_{LV} contains $\mathcal{O}(E^0)$ and $\mathcal{O}(E)$ terms.

Experimentally, effects of Lorentz violation on neutrino oscillations have been investigated in short-baseline neutrino beams [13–16], in long-baseline neutrino beams [17, 18], in reactor neutrinos at Double Chooz [19, 20], and in atmospheric neutrinos at IceCube [21] and Super-Kamiokande [22]. These experiments probe either the spectral anomalies of the oscillated neutrino flux or the sidereal variations of neutrino oscillation probabilities. In this paper, we

shall focus on LV effects to neutrino mixing angles and phases. As mentioned before, these effects grow with neutrino energies. Thus it is ideal to probe such effects through the flavor transitions of high energy astrophysical neutrinos. For simplicity, we only consider isotropic LV effects.

The observation of high energy astrophysical neutrinos by IceCube [23–26] is a significant progress in neutrino astronomy and provides new possibilities for testing neutrino properties. The first result by IceCube on the flavor composition of observed astrophysical neutrinos has been published in [27], and was updated in [28] by a combined-likelihood analysis taking into account more statistics. Meanwhile, independent efforts have been made to determine neutrino flavor compositions from IceCube data [29–31, 34]. As we shall see in latter sections, the flavor measurement in [28] is able to constrain H_{LV} more stringently than the previous experiments if the detected high energy neutrinos are produced from a special class of astrophysical sources. However, for more general astrophysical sources, the constraining power of the above measurement diminishes. Fortunately there is an active plan for extending the current IceCube detector to a larger volume, which is referred to as IceCube-Gen2 [35, 36]. This extension shall increase the effective area of the current 86-string detector up to a factor of 5. The expected improvement on neutrino flavor discrimination by IceCube-Gen2 has been studied in [37]. Using this result, we shall study sensitivities of IceCube-Gen2 to the parameters of H_{LV} .

Astrophysical neutrinos are commonly produced by either pp or $p\gamma$ collisions at astrophysical sources. For sufficiently high energies, pp collisions produce equal number of π^+ and π^- , which decay to neutrinos through $\pi^+ \rightarrow \mu^+ + \nu_\mu \rightarrow e^+ + \nu_\mu + \nu_e + \bar{\nu}_\mu$ and $\pi^- \rightarrow \mu^- + \bar{\nu}_\mu \rightarrow e^- + \bar{\nu}_\mu + \bar{\nu}_e + \nu_\mu$. This leads approximately to the flux ratio $\Phi^0(\nu_e) : \Phi^0(\nu_\mu) : \Phi^0(\nu_\tau) = 1/3 : 2/3 : 0$ for both neutrinos and anti-neutrinos. Here $\Phi^0(\nu_\alpha)$ denotes generically the flux of neutrino or anti-neutrino of flavor α . This type of source is referred to as the pion source. A more detailed study on the neutrino flavor fraction with the consideration of neutrino spectral index is given in [38]. For an E^{-2} spectrum, the neutrino flavor fraction at the source is $(f_e^0, f_\mu^0, f_\tau^0) = (0.35, 0.65, 0)$, where $f_\alpha^0 \equiv \Phi^0(\nu_\alpha)/(\Phi^0(\nu_e) + \Phi^0(\nu_\mu) + \Phi^0(\nu_\tau))$. However, for the purpose of this work, it suffices to take $(f_e^0, f_\mu^0, f_\tau^0) = (1/3, 2/3, 0)$. We note that the secondary muons in some astrophysical objects can lose energy quickly by synchrotron cooling in magnetic fields or interactions with matter before their decays. Hence the neutrino flavor fraction at the source becomes

(0, 1, 0). This type of source is referred to as the muon-damped source [31, 39–41]. The production mechanism of astrophysical neutrinos with $p\gamma$ collisions is more complicated. The leading process of this category is $p\gamma \rightarrow n\pi^+$ which gives rise to the flavor fraction (1/2, 1/2, 0) for neutrinos and (0, 1, 0) for anti-neutrinos. The sub-leading process is $p\gamma \rightarrow p\pi^+\pi^-$ which is non-negligible when the spectral index β of the target photon is harder than $\beta \sim 1$ [32, 33]. This process produces equal number of neutrinos and anti-neutrinos with a common flavor fraction (1/3, 2/3, 0). Since the flavor fraction of neutrinos produced by $p\gamma$ collisions is relatively uncertain, we shall only astrophysical neutrinos produced by pp collisions in our analysis.

We note that effects of new-physics Hamiltonian (with Lorentz violation as a special case), parametrized as $(E_\nu/\Lambda_n)^n U_n O_n U_n^\dagger$, to the flavor transitions of astrophysical neutrinos were discussed in [42, 43] for $n = 0$ and 1 (similar discussions were also given in [44–46]). The authors scan all possible structures of the mixing matrix U_n for given new-physics scales Λ_n and O_n and determine the allowed range of astrophysical neutrino flavor fractions on Earth resulting from the full Hamiltonian $H = H_{\text{SM}} + (E_\nu/\Lambda_n)^n U_n O_n U_n^\dagger$. In our work, we shall focus on LV effects which are parameterized in a different form from the above new-physics Hamiltonian. We shall discuss current and future constraints on LV effects by comparing the predicted neutrino flavor fractions with the measurement by the current IceCube detector [28] and that expected [37] in the future IceCube-Gen2 detector. Our results can be directly compared with previously most stringent constraints obtained by Super-Kamiokande [22].

This paper is organized as follows. In Sec. II, we incorporate LV effects into the full neutrino Hamiltonian in the framework of SME. We then study analytically the flavor transition of astrophysical neutrinos assuming the dominance of H_{LV} over H_{SM} . As stated before such a dominance is possible for high energy astrophysical neutrinos. We discuss constraints on LV effects by the current IceCube flavor measurement. Such discussions pave the way for detailed numerical studies in the next section. In Sec. III, we study the flavor transitions of astrophysical neutrinos with the full Hamiltonian $H = H_{\text{SM}} + H_{\text{LV}}$. The expected sensitivities of IceCube-Gen2 to H_{LV} are studied. We conclude in Sec. IV.

II. LORENTZ VIOLATION IN NEUTRINO OSCILLATIONS

Lorentz violation effects in neutrino oscillations are incorporated by introducing a Lorentz violation term H_{LV} in addition to the standard model neutrino Hamiltonian. Hence

$$H = H_{SM} + H_{LV}, \quad (1)$$

where $H_{SM} \equiv UM^2U^\dagger/2E$ is the standard model neutrino Hamiltonian in vacuum with M^2 the neutrino mass matrix

$$M^2 = \begin{pmatrix} 0 & 0 & 0 \\ 0 & \Delta m_{21}^2 & 0 \\ 0 & 0 & \Delta m_{31}^2 \end{pmatrix}, \quad (2)$$

U is the PMNS matrix. Here we do not consider matter effects to neutrino propagations inside the Earth. This is because we only focus on neutrino events with energies higher than few tens of TeV such that the Earth regeneration effect to the neutrino flavor transition is negligible. For neutrinos, the general form of LV Hamiltonian is given by

$$H_{LV}^\nu = \frac{p^\lambda}{E} \begin{pmatrix} a_{ee}^\lambda & a_{e\mu}^\lambda & a_{e\tau}^\lambda \\ a_{e\mu}^{\lambda*} & a_{\mu\mu}^\lambda & a_{\mu\tau}^\lambda \\ a_{e\tau}^{\lambda*} & a_{\mu\tau}^{\lambda*} & a_{\tau\tau}^\lambda \end{pmatrix} - \frac{p^\rho p^\lambda}{E} \begin{pmatrix} c_{ee}^{\rho\lambda} & c_{e\mu}^{\rho\lambda} & c_{e\tau}^{\rho\lambda} \\ c_{e\mu}^{\rho\lambda*} & c_{\mu\mu}^{\rho\lambda} & c_{\mu\tau}^{\rho\lambda} \\ c_{e\tau}^{\rho\lambda*} & c_{\mu\tau}^{\rho\lambda*} & c_{\tau\tau}^{\rho\lambda} \end{pmatrix}. \quad (3)$$

Since we shall only consider isotropic LV effects, H_{LV}^ν in this simplification reduces to [10]

$$H_{LV}^\nu = \begin{pmatrix} a_{ee}^T & a_{e\mu}^T & a_{e\tau}^T \\ a_{e\mu}^{T*} & a_{\mu\mu}^T & a_{\mu\tau}^T \\ a_{e\tau}^{T*} & a_{\mu\tau}^{T*} & a_{\tau\tau}^T \end{pmatrix} - \frac{4E}{3} \begin{pmatrix} c_{ee}^{TT} & c_{e\mu}^{TT} & c_{e\tau}^{TT} \\ c_{e\mu}^{TT*} & c_{\mu\mu}^{TT} & c_{\mu\tau}^{TT} \\ c_{e\tau}^{TT*} & c_{\mu\tau}^{TT*} & c_{\tau\tau}^{TT} \end{pmatrix}, \quad (4)$$

where T is the time component of Sun-centered celestial equatorial frame (T, X, Y, Z).

For anti-neutrinos, we have

$$H_{LV}^{\bar{\nu}} = - \begin{pmatrix} a_{ee}^T & a_{e\mu}^T & a_{e\tau}^T \\ a_{e\mu}^{T*} & a_{\mu\mu}^T & a_{\mu\tau}^T \\ a_{e\tau}^{T*} & a_{\mu\tau}^{T*} & a_{\tau\tau}^T \end{pmatrix}^* - \frac{4E}{3} \begin{pmatrix} c_{ee}^{TT} & c_{e\mu}^{TT} & c_{e\tau}^{TT} \\ c_{e\mu}^{TT*} & c_{\mu\mu}^{TT} & c_{\mu\tau}^{TT} \\ c_{e\tau}^{TT*} & c_{\mu\tau}^{TT*} & c_{\tau\tau}^{TT} \end{pmatrix}^*. \quad (5)$$

Diagonalizing the full Hamiltonian in Eq. (1) yields a new mass-flavor mixing matrix V . The neutrino flavor transition probability is then given by

$$P_{\alpha\beta} = \delta_{\alpha\beta} - 4 \sum_{j>i} \Re(V_{\beta j} V_{\beta i}^* V_{\alpha j}^* V_{\alpha i}) \sin^2(L\Delta E_{ji}/2) + 2 \sum_{j>i} \Im(V_{\beta j} V_{\beta i}^* V_{\alpha j}^* V_{\alpha i}) \sin^2(L\Delta E_{ji}), \quad (6)$$

where $\Delta E_{ji} \equiv E_j - E_i$ is the difference between the energy eigenvalues. For high-energy astrophysical neutrinos, L is so large that the rapid oscillating terms are averaged so that

$$P_{\alpha\beta} = \sum_{i=1}^3 |V_{\alpha i}|^2 |V_{\beta i}|^2. \quad (7)$$

Since $P_{\alpha\beta}$ depends only on the elements of V , the neutrino flavor composition observed on the Earth for a given astrophysical neutrino source is affected by LV parameters. Therefore, the measurement of neutrino flavor fraction by neutrino telescopes such as IceCube is useful for constraining LV parameters. For convenience in discussions, we shall first focus on constraints to $a_{\alpha\beta}^T$ by setting $c_{\alpha\beta}^{TT} = 0$. The constraints to $c_{\alpha\beta}^{TT}$ will be commented later.

Recently, Super-Kamiokande [22] has placed upper limits on $|a_{\alpha\beta}^T|$ of the order 10^{-23} GeV. With $|a_{\alpha\beta}^T|$ of this energy scale, it is interesting to note that $\Delta m_{ij}^2/E$ is smaller than $|a_{\alpha\beta}^T|$ by about 3 orders of magnitude for neutrino energy of a few tens of TeV. Hence for neutrino events analyzed by IceCube for flavor measurement [28], the LV term H_{LV} dominates over the standard model Hamiltonian $UM^2U^\dagger/2E$ if any of the $a_{\alpha\beta}^T$ terms is set to be at the SK limit, $\sim 10^{-23}$ GeV. Therefore, to investigate IceCube constraints on $a_{\alpha\beta}^T$, it is useful to begin with the approximation $H \approx H_{LV}^{\nu,\bar{\nu}}$, i.e., neglecting $UM^2U^\dagger/2E$.

Even by considering $H_{LV}^{\nu,\bar{\nu}}$ alone, it is still rather cumbersome to analytically diagonalize the Hamiltonian and calculate the transition probability $P_{\alpha\beta}$. In this section, we focus on special patterns of $H_{LV}^{\nu,\bar{\nu}}$ and calculate their corresponding flavor transition probabilities $P_{\alpha\beta}$. Results from these special scenarios are helpful for us to perform detailed numerical studies in the next session.

A. Only $a_{e\mu}^T$ and $a_{e\mu}^{T*}$ are non-vanishing

We first consider a special pattern that only $a_{e\mu}^T$ and $a_{e\mu}^{T*}$ are non-vanishing in $H_{LV}^{\nu,\bar{\nu}}$. For neutrinos, one can easily diagonalize H_{LV}^ν and obtain the transition probability matrix

$$P = \begin{pmatrix} 1/2 & 1/2 & 0 \\ 1/2 & 1/2 & 0 \\ 0 & 0 & 1 \end{pmatrix}. \quad (8)$$

It is easy to show that the diagonalization of $H_{LV}^{\bar{\nu}}$ also leads to the same transition probability matrix. With an identical transition probability matrix for neutrinos and anti-neutrinos, we

note that the flavor fraction of $\nu + \bar{\nu}$ flux on the Earth is $(1/2, 1/2, 0)$ for the pion source. For the muon damped source, this transition probability matrix also gives rise to the same flavor fraction of $\nu + \bar{\nu}$ flux on the Earth coincidentally. This flavor fraction is within the 68% confidence region of the current IceCube measurement as shown in Fig. 1. In this figure we also show the expected sensitivities of IceCube-Gen2 from Ref. [37], which is based upon 10 years of exposure to astrophysical neutrinos from the pion type of sources with energies beyond 100 TeV in a $E^{-2.2}$ spectrum.

B. Only $a_{e\tau}^T$ and $a_{e\tau}^{T*}$ are non-vanishing

We next consider a special pattern that only $a_{e\tau}^T$ and $a_{e\tau}^{T*}$ are non-vanishing in $H_{LV}^{\nu,\bar{\nu}}$. The transition probability matrix in this case can be easily inferred from the previous case with the interchange $\mu \leftrightarrow \tau$. Hence

$$P = \begin{pmatrix} 1/2 & 0 & 1/2 \\ 0 & 1 & 0 \\ 1/2 & 0 & 1/2 \end{pmatrix}, \quad (9)$$

for both neutrinos and anti-neutrinos. With the transition probability matrix given by Eq. (9), the flavor fraction of $\nu + \bar{\nu}$ flux on the Earth is $(1/6, 2/3, 1/6)$ for the pion source and $(0, 1, 0)$ for the muon damped source as shown in Fig. 1. For the case of pion source, the flavor fraction on the Earth is at the boundary of current IceCube 95% confidence region. For the muon-damped source, the flavor fraction on the Earth is disfavored by current IceCube with more than 2σ significance.

C. Only $a_{\mu\tau}^T$ and $a_{\mu\tau}^{T*}$ are non-vanishing

We next consider a special pattern that only $a_{\mu\tau}^T$ and $a_{\mu\tau}^{T*}$ are non-vanishing in $H_{LV}^{\nu,\bar{\nu}}$. In such a case, the transition probability is

$$P = \begin{pmatrix} 1 & 0 & 0 \\ 0 & 1/2 & 1/2 \\ 0 & 1/2 & 1/2 \end{pmatrix}, \quad (10)$$

for both neutrinos and anti-neutrinos. It is easily seen that this matrix differs from previous one by the interchange $e \leftrightarrow \tau$ as it should be. With such a transition matrix, the flavor

fraction of $\nu + \bar{\nu}$ flux on the Earth is $(1/3, 1/3, 1/3)$ for pion source and $(0, 1/2, 1/2)$ for the muon-damped source, respectively. The former lies on the boundary of 68% confidence region of IceCube measurement while the latter is within the 95% confidence region as shown in Fig. 1.

D. Only diagonal elements are non-vanishing

Since the flavor transition probability only depends on the differences of diagonal elements, one can take the non-vanishing diagonal elements as $a_{\mu\mu}^T$ and $a_{\tau\tau}^T$ while setting $a_{ee}^T = 0$ without losing the generality. In this case, the eigenvectors of $H_{LV}^{\nu,\bar{\nu}}$ are $(1, 0, 0)$, $(0, 1, 0)$, and $(0, 0, 1)$ such that $P = I$. We have assumed $a_{\mu\mu}^T \neq a_{\tau\tau}^T$ to avoid the degeneracy of energy eigenvalues or else the decoherent limit such as Eq. (7) is not well defined. Hence the neutrino flavor ratio on the Earth is $(1/3, 2/3, 0)$ for the pion source and $(0, 1, 0)$ for the muon-damped source. The former is within the IceCube 95% confidence region while the latter is out of this region similar to the case B.

From the above special cases of $H_{LV}^{\nu,\bar{\nu}}$, one can see that the case B is at the highest tension with the current IceCube measurement, particularly if all the detected neutrino events are from the muon-damped source. On the other hand, the case C is in the best agreement with the current data.

In the next section, we shall perform detailed analyses, which include considering deviations to the special patterns of $H_{LV}^{\nu,\bar{\nu}}$ and taking into account the effects of H_{SM} . We shall assume the simplest scenario that all the astrophysical neutrinos are produced by the pion source. This is also the conservative assumption since the predictions by $H_{LV}^{\nu,\bar{\nu}}$ with the pion source are less constrained by the current IceCube data as one can see from Fig. 1. With such type of source, the left panel of Fig. 1 shows that only the case B is slightly out of the IceCube 2σ confidence region. A slight deviation to such a pattern would certainly give rise to neutrino flavor fractions in good agreements with the data. Therefore a stringent constraint to $H_{LV}^{\nu,\bar{\nu}}$ requires IceCube-Gen2. This is our main target of study in the coming session.

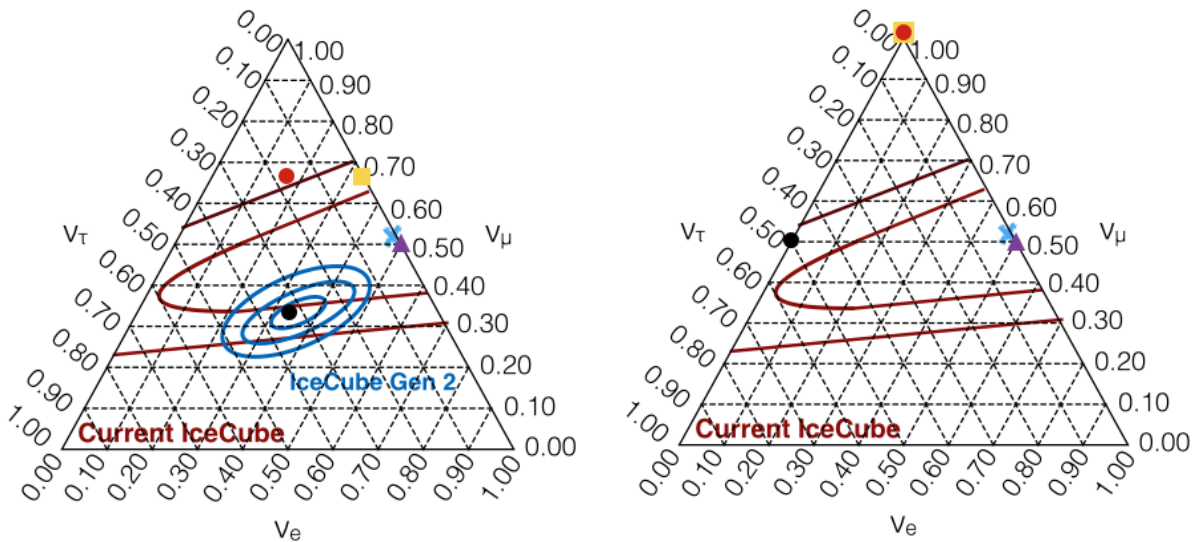


FIG. 1: The flavor fractions of astrophysical neutrinos arriving on Earth. The left panel is for the pion source while the right panel is for the muon-damped source. Regions inside the brown lines are the current IceCube measurements (independent of astrophysical sources) with the blue cross denoting the best fit values [28]. Regions inside the blue curves are the IceCube-Gen2 $1\sigma - 3\sigma$ sensitivity regions (available only for the pion source) given in [37]. The predicted flavor fractions on Earth assuming the dominance of Lorentz violating Hamiltonian $H_{LV}^{\nu,\bar{\nu}}$ are denoted by the purple triangle, the red dot, the black dot, and the yellow square for the special scenarios of $|a_{e\mu}^T| \neq 0$, $|a_{e\tau}^T| \neq 0$, $|a_{\mu\tau}^T| \neq 0$, and $a_{\mu\mu,\tau\tau}^T \neq 0$, respectively.

III. THE SENSITIVITY OF ICECUBE-GEN2 IN PROBING THE LORENTZ VIOLATION PARAMETERS

In this section, we apply the projected flavor discrimination sensitivity of IceCube-Gen2 [37] to estimate the future constraints on Lorentz violation parameters. In the above projected sensitivity, only the pion source produced by pp collisions is considered. Therefore we shall only consider this type of source in the following discussions. From Fig. 1, we note that the predictions by all the special LV patterns except the one with $|a_{\mu\tau}^T| \neq 0$ are outside of the projected 3σ confidence region of IceCube-Gen2. Hence we will consider deviations to such patterns of $H_{LV}^{\nu,\bar{\nu}}$ together with the contributions from H_{SM} for generating the predictions to neutrino flavor compositions. In our numerical studies, the neutrino mixing

parameters in H_{SM} are taken from [47]. The neutrino energy appearing in H_{SM} should in principle follow the $E^{-2.2}$ distribution with the threshold at 100 TeV according to Ref. [37]. However, for simplicity, we fix $E = 100$ TeV. This is a conservative choice that makes H_{LV}^ν least dominant compared to H_{SM} . Let us begin with the case that $a_{e\mu}^T$ dominates all the other elements in magnitudes.

A. $|a_{e\mu}^T|$ dominance

To determine how IceCube-Gen2 may constrain such a scenario, we first choose a value for $|a_{e\mu}^T|$ that is lower than the current experimental limit, and allow other elements in $H_{\text{LV}}^{\nu,\bar{\nu}}$ to grow. We increase the ratio $|a_{\alpha\beta}^T|/|a_{e\mu}^T|$ for each matrix element $a_{\alpha\beta}^T$ until the predicted neutrino flavor fraction on the Earth touches the projected 3σ boundary of IceCube-Gen2. To simplify the parameter scanning, we have taken the upper limit of $|a_{e\tau}^T|$ identical to that of $|a_{\mu\tau}^T|$ and the upper limit of $|a_{\mu\mu}^T|$ identical to that of $|a_{\tau\tau}^T|$. Initially we allow all the parameters to grow into the same upper limit in absolute values until the above mentioned 3σ boundary is touched. We then allow $|a_{\mu\mu}^T|$ and $|a_{\tau\tau}^T|$ to grow further since $P_{\alpha\beta}$ is less sensitive to the growth of these two parameters. It is understood that such a scanning procedure will not identify the full disfavored parameter space. However the result is sufficient to tell us how well IceCube-Gen2 can constrain $H_{\text{LV}}^{\nu,\bar{\nu}}$ in the future. We note that the above scanning procedure produces the same constrained parameter region for neutrinos and anti-neutrinos. There are two reasons for this. First, for the pion source due to pp collisions, there are equal numbers of neutrinos and anti-neutrinos produced with a common flavor fraction. Second, by comparing Eqs. (4) and (5), one realizes that the study of anti-neutrino flavor transitions constrains $|-a_{\alpha\beta}^T|$, which is the same as the study of neutrino flavor transitions that constrains $|a_{\alpha\beta}^T|$.

The current 95% C.L. limits for $a_{e\mu}^T$ are $\text{Re}(a_{e\mu}^T) < 1.8 \times 10^{-23}$ GeV and $\text{Im}(a_{e\mu}^T) < 1.8 \times 10^{-23}$ GeV, respectively [22]. For our following studies, we shall take $|a_{e\mu}^T|$ as 5×10^{-24} GeV and 5×10^{-25} GeV, respectively. The black region in each plot of Fig. 2 is disfavored by IceCube-Gen2 at 3σ . The black region in the left plot is generated by fixing $|a_{e\mu}^T|$ at 5×10^{-24} GeV while varying the other LV parameters within the range given by the second column of Table I. In other words, the parameter ranges that generate the black region in this plot are $0 \leq |a_{e\tau}^T|/|a_{e\mu}^T| \leq 0.24$, $0 \leq |a_{\mu\tau}^T|/|a_{e\mu}^T| \leq 0.24$, $0 \leq |a_{\mu\mu}^T|/|a_{e\mu}^T| \leq 0.30$, and

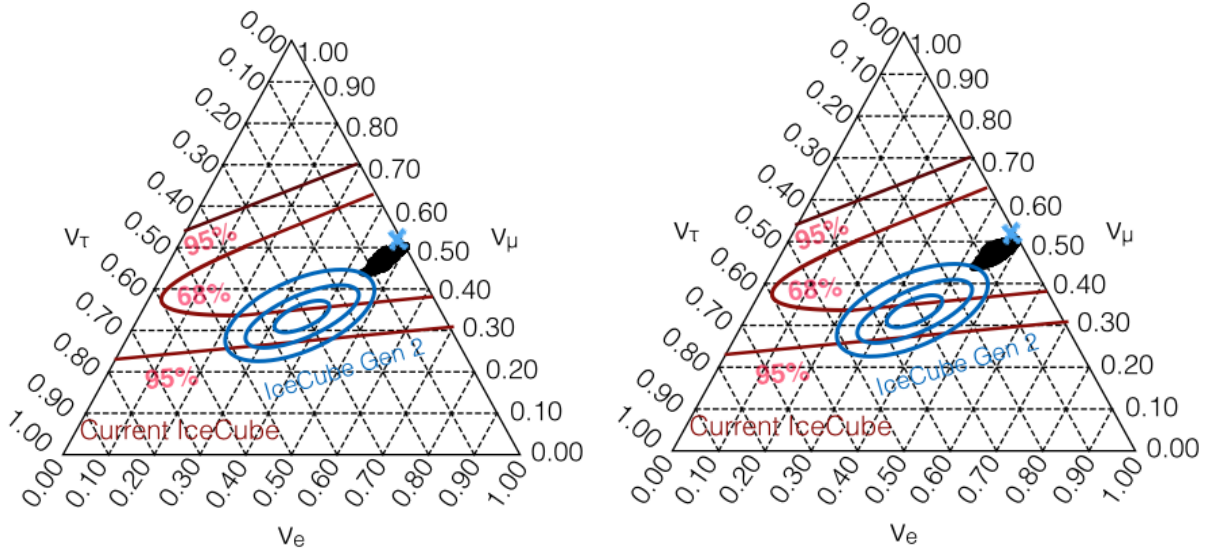


FIG. 2: The black region in each plot is disfavored by IceCube-Gen2 at 3σ . The black region in the left plot corresponds to $|a_{e\mu}^T| = 5 \times 10^{-24}$ GeV with $0 \leq |a_{e\tau}^T|/|a_{e\mu}^T| \leq 0.24$, $0 \leq |a_{\mu\tau}^T|/|a_{e\mu}^T| \leq 0.24$, $0 \leq |a_{\mu\mu}^T|/|a_{e\mu}^T| \leq 0.30$, and $0 \leq |a_{\tau\tau}^T|/|a_{e\mu}^T| \leq 0.30$ as can be seen from the second column of Table I. The black region in the right plot corresponds to $|a_{e\mu}^T| = 5 \times 10^{-25}$ GeV with the ranges of other LV parameters given by the third column of Table I.

$0 \leq |a_{\tau\tau}^T|/|a_{e\mu}^T| \leq 0.30$. The black region in the right plot is generated by fixing $|a_{e\mu}^T|$ at 5×10^{-25} GeV while varying the other LV parameters within the range given by the third column of Table I.

$ a_{e\mu}^T $	5×10^{-24} GeV	5×10^{-25} GeV
$ a_{e\tau}^T / a_{e\mu}^T $	(0, 0.24)	(0, 0.23)
$ a_{\mu\tau}^T / a_{e\mu}^T $	(0, 0.24)	(0, 0.23)
$ a_{\mu\mu}^T / a_{e\mu}^T $	(0, 0.30)	(0, 0.26)
$ a_{\tau\tau}^T / a_{e\mu}^T $	(0, 0.30)	(0, 0.26)

TABLE I: The disfavored ranges of LV parameters expected by IceCube-Gen2 for $|a_{e\mu}^T|$ dominance scenario. Taking the second column as an example, for $|a_{e\mu}^T| = 5 \times 10^{-24}$ GeV, the disfavored LV parameter ranges for astrophysical neutrinos are $0 \leq |a_{e\tau}^T|/|a_{e\mu}^T| \leq 0.24$, $0 \leq |a_{\mu\tau}^T|/|a_{e\mu}^T| \leq 0.24$, $0 \leq |a_{\mu\mu}^T|/|a_{e\mu}^T| \leq 0.30$, and $0 \leq |a_{\tau\tau}^T|/|a_{e\mu}^T| \leq 0.30$.

B. $|a_{e\tau}^T|$ dominance

The current 95% C.L. limits for $a_{e\tau}^T$ are $\text{Re}(a_{e\tau}^T) < 4.1 \times 10^{-23}$ GeV and $\text{Im}(a_{e\tau}^T) < 2.8 \times 10^{-23}$ GeV, respectively [22]. As in the previous case, we also choose $|a_{e\tau}^T|$ to be 5×10^{-24} GeV, and 5×10^{-25} GeV, respectively. Once again we work out the expected ranges of LV parameters to be highly constrained by IceCube-Gen2. The results are shown in Fig. 3 and Table II. It is found that the disfavored parameter ranges in the $|a_{e\tau}^T|$ dominance scenario are larger than those in the $|a_{e\mu}^T|$ dominance scenario.

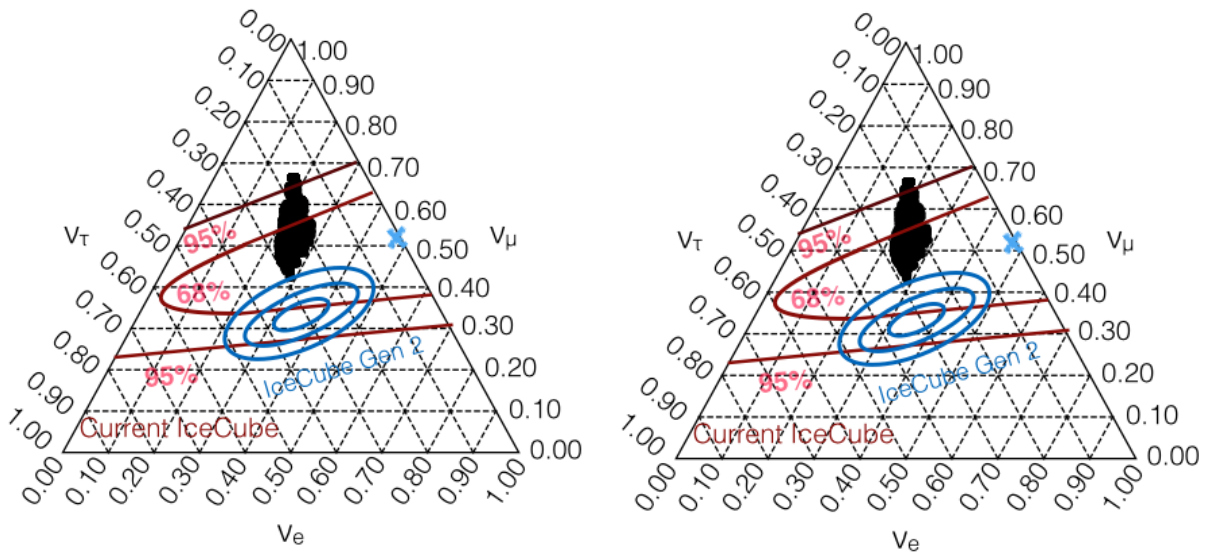


FIG. 3: The black region in each plot is disfavored by IceCube-Gen2 at 3σ . The plots are arranged in the same way as the previous figure. The ranges of LV parameters corresponding to each black region are summarized in Table II.

$ a_{e\tau}^T $	5×10^{-24} GeV	5×10^{-25} GeV
$ a_{e\mu}^T / a_{e\tau}^T $	(0, 0.42)	(0, 0.39)
$ a_{\mu\tau}^T / a_{e\tau}^T $	(0, 0.42)	(0, 0.39)
$ a_{\mu\mu}^T / a_{e\tau}^T $	(0, 0.50)	(0, 0.45)
$ a_{\tau\tau}^T / a_{e\tau}^T $	(0, 0.50)	(0, 0.45)

TABLE II: The disfavored ranges of LV parameters expected by IceCube-Gen2 for $|a_{e\tau}^T|$ dominance scenario.

C. Diagonal dominance

As mentioned earlier, one can set $|a_{ee}^T|$ to zero without the generality. We have also assumed $|a_{\mu\mu}^T| \neq |a_{\mu\mu}^T|$ to avoid the degeneracy of energy eigenvalues in $H_{LV}^{\nu,\bar{\nu}}$. We choose $a_{\mu\mu}^T = 2a_{\tau\tau}^T$ and $a_{\mu\mu}^T = -2a_{\tau\tau}^T$ for illustrating the diagonal dominance scenario. The constraints on diagonal elements of $H_{LV}^{\nu,\bar{\nu}}$ are not studied in Ref. [22]. To study these constraints, we again take $a_{\mu\mu}^T$ as 5×10^{-24} GeV and 5×10^{-25} GeV, respectively. The LV parameter ranges expected to be constrained by IceCube-Gen2 are shown in Fig. 4 and Table III for $a_{\mu\mu}^T = 2a_{\tau\tau}^T$. The results with $a_{\mu\mu}^T = -2a_{\tau\tau}^T$ are presented in Fig. 5 and Table IV.

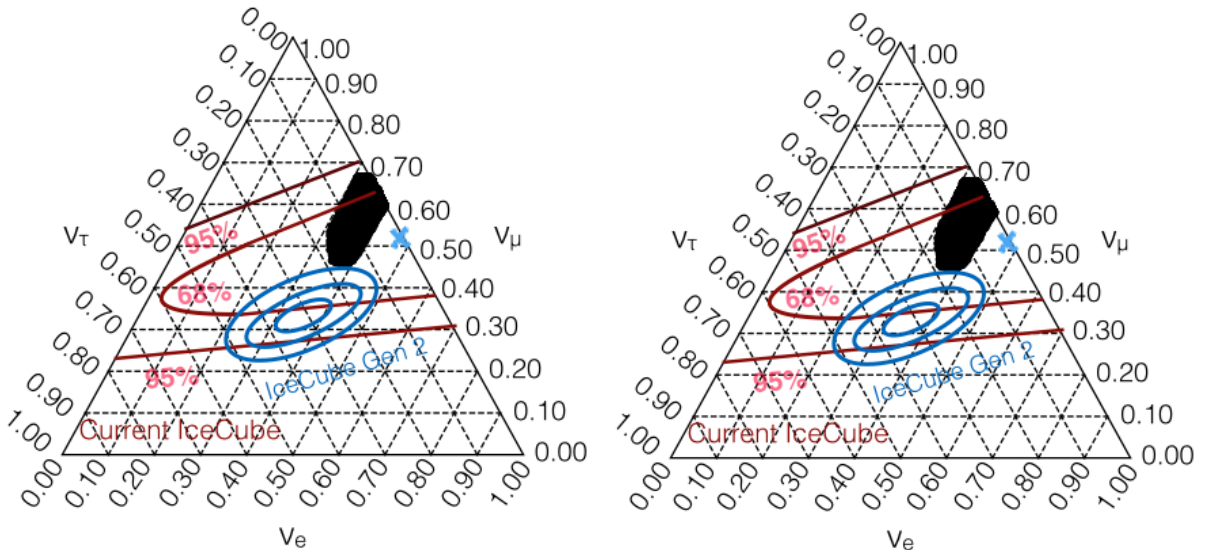


FIG. 4: The black region in each plot is disfavored by IceCube-Gen2 at 3σ . The plots are arranged in the same way as the previous figure. The ranges of LV parameters corresponding to each black region are summarized in Table III.

$a_{\mu\mu}^T = 2a_{\tau\tau}^T$	5×10^{-24} GeV	5×10^{-25} GeV
$ a_{e\mu}^T / a_{\mu\mu}^T $	(0, 0.40)	(0, 0.39)
$ a_{e\tau}^T / a_{\mu\mu}^T $	(0, 0.40)	(0, 0.39)
$ a_{\mu\tau}^T / a_{\mu\mu}^T $	(0, 0.40)	(0, 0.39)

TABLE III: The disfavored ranges of LV parameters expected by IceCube-Gen2 for diagonal dominance scenario with $a_{\mu\mu}^T = 2a_{\tau\tau}^T$.

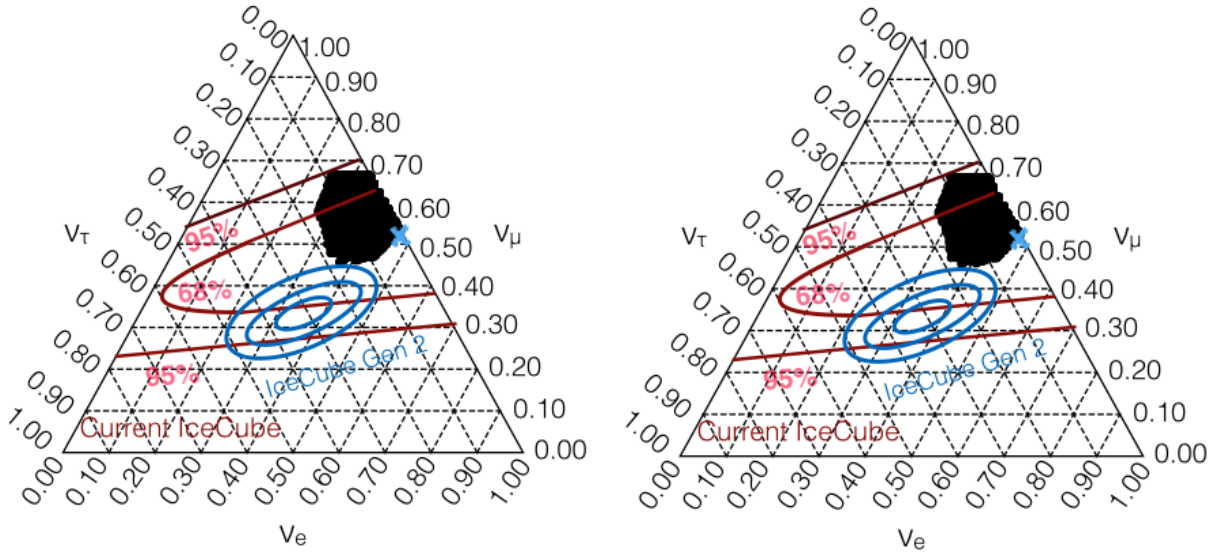


FIG. 5: The black region in each plot is disfavored by IceCube-Gen2 at 3σ . The plots are arranged in the same way as the previous figure. The ranges of LV parameters corresponding to each black region are summarized in Table IV.

$a_{\mu\mu}^T = -2a_{\tau\tau}^T$	5×10^{-24} GeV	5×10^{-25} GeV
$ a_{e\mu}^T / a_{\mu\mu}^T $	(0, 1)	(0, 1)
$ a_{e\tau}^T / a_{\mu\mu}^T $	(0, 1)	(0, 1)
$ a_{\mu\tau}^T / a_{\mu\mu}^T $	(0, 1)	(0, 1)

TABLE IV: The disfavored ranges of LV parameters expected by IceCube-Gen2 for diagonal dominance scenario with $a_{\mu\mu}^T = -2a_{\tau\tau}^T$.

For $a_{\mu\mu}^T = 2a_{\tau\tau}^T$, the LV parameter ranges expected to be ruled out by IceCube-Gen2 are $0 \leq |a_{e\mu}^T|/|a_{\mu\mu}^T| \leq 0.40$, $0 \leq |a_{e\tau}^T|/|a_{\mu\mu}^T| \leq 0.40$, and $0 \leq |a_{\mu\tau}^T|/|a_{\mu\mu}^T| \leq 0.40$ for $|a_{\mu\mu}^T| = 5 \times 10^{-24}$ GeV. The disfavored parameter ranges are almost the same for $|a_{\mu\mu}^T| = 5 \times 10^{-25}$ GeV. On the other hand, for $a_{\mu\mu}^T = -2a_{\tau\tau}^T$, much larger LV parameter ranges can be ruled out, i.e., $0 \leq |a_{e\mu}^T|/|a_{\mu\mu}^T| \leq 1$, $0 \leq |a_{e\tau}^T|/|a_{\mu\mu}^T| \leq 1$, and $0 \leq |a_{\mu\tau}^T|/|a_{\mu\mu}^T| \leq 1$. In principle the disfavored LV parameter ranges could also include $|a_{\alpha\beta}^T|/|a_{\mu\mu}^T| > 1$ for any non-diagonal element $a_{\alpha\beta}^T$. However, since we have assumed diagonal dominance, we terminate the parameter scan at $|a_{\alpha\beta}^T|/|a_{\mu\mu}^T| = 1$.

So far we have only discussed IceCube-Gen2 sensitivities to $a_{\alpha\beta}^T$. One can also study the

sensitivities to dimensionless parameters $c_{\alpha\beta}^{TT}$ by turning off $a_{\alpha\beta}^T$. In fact, the sensitivities to $c_{\alpha\beta}^{TT}$ can be inferred from the sensitivities to $a_{\alpha\beta}^T$. Obviously $-4E c_{\alpha\beta}^{TT}/3$ replaces $a_{\alpha\beta}^T$ when the latter is turned off. Hence, taking $c_{e\mu}^{TT}$ dominance as an example, one infers from the results of $a_{e\mu}^T$ dominance that, for $4E|c_{e\mu}^{TT}|/3 = 5 \times 10^{-24}$ GeV, the LV parameter ranges $0 \leq |c_{e\tau}^{TT}|/|c_{e\mu}^{TT}| \leq 0.24$, $0 \leq |c_{\mu\tau}^{TT}|/|c_{e\mu}^{TT}| \leq 0.24$, $0 \leq |c_{\mu\mu}^{TT}|/|c_{e\mu}^{TT}| \leq 0.30$, and $0 \leq |c_{\tau\tau}^{TT}|/|c_{e\mu}^{TT}| \leq 0.30$ can be ruled out at 3σ by IceCube-Gen2. We note that the 3σ region given by Ref. [37] is obtained by setting the threshold energy of astrophysical neutrinos at 100 TeV. Hence the condition $4E|c_{e\mu}^{TT}|/3 = 5 \times 10^{-24}$ GeV would correspond to $|c_{e\mu}^{TT}|$ no larger than 3.8×10^{-29} . Such a sensitivity to $|c_{e\mu}^{TT}|$ is far beyond the reach of SuperKamiokande [22] which gives the upper limits $\text{Re}(c_{e\mu}^{TT}) < 8.0 \times 10^{-27}$ and $\text{Im}(c_{e\mu}^{TT}) < 8.0 \times 10^{-27}$. Even if we push $|c_{e\mu}^{TT}|$ down to 3.8×10^{-30} , one can still rule out LV parameter ranges characterized by $0 \leq |c_{e\tau}^{TT}|/|c_{e\mu}^{TT}| \leq 0.23$, $0 \leq |c_{\mu\tau}^{TT}|/|c_{e\mu}^{TT}| \leq 0.23$, $0 \leq |c_{\mu\mu}^{TT}|/|c_{e\mu}^{TT}| \leq 0.26$, and $0 \leq |c_{\tau\tau}^{TT}|/|c_{e\mu}^{TT}| \leq 0.26$. Clearly the disfavored LV parameter ranges for $|c_{e\mu}^{TT}|$ dominance scenario and diagonal dominance scenario can be obtained in the similar way.

IV. DISCUSSIONS AND CONCLUSIONS

In this paper, we discuss the sensitivities of future IceCube-Gen2 to Lorentz violation parameters in the neutrino sector. We consider astrophysical neutrinos from the pion source caused by pp collisions. In such a case, there are equal numbers of neutrinos and anti-neutrinos produced with the flavor fraction $(1/3, 2/3, 0)$ at the source for both neutrinos and anti-neutrinos. Taking $f_\alpha \equiv \Phi(\nu_\alpha)/(\Phi(\nu_e)+\Phi(\nu_\mu)+\Phi(\nu_\tau))$ as the neutrino flavor fraction on the Earth, we have $f_e = P_{ee}/3 + 2P_{e\mu}/3$. Since $P_{\alpha\beta} = P_{\beta\alpha}$ still holds with the addition of LV Hamiltonian, we have $P_{ee} = 1 - P_{\mu e} - P_{\tau e} = 1 - P_{e\mu} - P_{e\tau}$. Hence $f_e = 1/3 + (P_{e\mu} - P_{e\tau})/3$. Similarly we can show that $f_\mu = 1/3 + (P_{\mu\mu} - P_{\mu\tau})/3$, and $f_\tau = 1/3 + (P_{\mu\tau} - P_{\tau\tau})/3$. Clearly for astrophysical neutrinos arising from the pion source, the deviation of their flavor fraction to $(1/3, 2/3, 0)$ is solely due to $\mu - \tau$ symmetry breaking in the transition probability matrix.

For the standard model Hamiltonian H_{SM} , the $\mu - \tau$ symmetry breaking effects are small. To leading orders in $\cos 2\theta_{23}$ and $\sin \theta_{13}$, one has $(P_{e\mu} - P_{e\tau}) = 2\epsilon$, $(P_{\mu\mu} - P_{\mu\tau}) = (P_{\mu\tau} - P_{\tau\tau}) = -\epsilon$ with $\epsilon = 2 \cos 2\theta_{23}/9 + \sqrt{2} \sin \theta_{13} \cos \delta/9$ (taking $\sin^2 \theta_{12} = 1/3$) [48] where δ is the CP violation phase. Hence LV effects can be detectable provided they introduce sizable $\mu - \tau$

symmetry-breaking effects in the neutrino flavor transition matrix. In the case that only $a_{e\mu}^T$ and $a_{e\mu}^{T*}$ are non-vanishing in $H_{LV}^{\nu,\bar{\nu}}$, Eq. (8) gives $(P_{e\mu} - P_{e\tau}) = (P_{\mu\mu} - P_{\mu\tau}) = 1/2$ and $(P_{\mu\tau} - P_{\tau\tau}) = -1$. In this case, the resulting flavor fraction of astrophysical neutrinos arriving on Earth deviates significantly from $(1/3, 1/3, 1/3)$. Therefore we study the scenario of $|a_{e\mu}^T|$ dominance in $H_{LV}^{\nu,\bar{\nu}}$ and derive the sensitivity of future IceCube-Gen2 to such class of LV Hamiltonian. Similarly, in the case that only $a_{e\tau}^T$ and $a_{e\tau}^{T*}$ are non-vanishing in $H_{LV}^{\nu,\bar{\nu}}$, Eq. (9) gives $(P_{e\mu} - P_{e\tau}) = (P_{\mu\tau} - P_{\tau\tau}) = -1/2$ and $(P_{\mu\mu} - P_{\mu\tau}) = 1$. Hence the sensitivity of future IceCube-Gen2 to the $|a_{e\tau}^T|$ dominance scenario has been studied as well. We also study the diagonal dominance scenario of $H_{LV}^{\nu,\bar{\nu}}$ which contains only two non-vanishing matrix elements $a_{\mu\mu}^T$ and $a_{\tau\tau}^T$ (a_{ee}^T can be set to zero without losing the generality) in the extreme limit of this scenario. We have assumed $a_{\mu\mu}^T \neq a_{\tau\tau}^T$ to avoid the degeneracy in eigenvalues of $H_{LV}^{\nu,\bar{\nu}}$. The neutrino flavor transition matrix is an identity matrix in this case, which gives $(P_{e\mu} - P_{e\tau}) = 0$, $(P_{\mu\mu} - P_{\mu\tau}) = 1$, and $(P_{\mu\tau} - P_{\tau\tau}) = -1$. Once more the $\mu - \tau$ symmetry-breaking effects are large and the sensitivity of future IceCube-Gen2 to such class of LV Hamiltonian was also studied. Finally we do not study further the scenario of $|a_{\mu\tau}^T|$ dominance. In the extreme limit that only $a_{\mu\tau}^T$ and $a_{\mu\tau}^{T*}$ are non-vanishing in $H_{LV}^{\nu,\bar{\nu}}$, the $\mu - \tau$ symmetry is precisely respected as Eq. (10) implies.

In summary, we have taken a phenomenological approach that incorporate all LV effects in the neutrino sector with a set of local operators [3–7]. To simplify our discussions, we consider only the isotropic LV effects [10], so that the structure of LV Hamiltonian is given by Eqs. (4) and (5). We have worked out the sensitivities of IceCube-Gen2 to the dimensionful LV parameters $a_{\alpha\beta}^T$ and the dimensionless LV parameters $C_{\alpha\beta}^{TT}$, respectively. Our approach focuses on constraining some specific flavor structures of LV Hamiltonian using anticipated sensitivities of IceCube-Gen2 to the flavor fraction of high energy astrophysical neutrinos. These expected constraints differ from previous ones which only impose limit on each individual matrix element of $H_{LV}^{\nu,\bar{\nu}}$ while setting all the other matrix elements to zero. We have also shown that the expected IceCube-Gen2 constraints to $a_{\alpha\beta}^T$ and $C_{\alpha\beta}^{TT}$ could be better than the current bounds [22] by at least two orders of magnitudes.

ACKNOWLEDGEMENTS

This work is supported by Ministry of Science and Technology, Taiwan under Grant No. 105-2112-M-009 -014.

- [1] V. A. Kostelecky and S. Samuel, *Phys. Rev. D* **39**, 683 (1989).
- [2] V. A. Kostelecky and R. Potting, *Nucl. Phys. B* **359**, 545 (1991).
- [3] D. Colladay and V. A. Kostelecky, *Phys. Rev. D* **55**, 6760 (1997).
- [4] D. Colladay and V. A. Kostelecky, *Phys. Rev. D* **58**, 116002 (1998).
- [5] V. A. Kostelecky, *Phys. Rev. D* **69**, 105009 (2004).
- [6] G. Amelino-Camelia, C. Lammerzahl, A. Macias and H. Muller, *AIP Conf. Proc.* **758**, 30 (2005).
- [7] R. Bluhm, *Lect. Notes Phys.* **702**, 191 (2006).
- [8] V. A. Kostelecky and N. Russell, *Rev. Mod. Phys.* **83**, 11 (2011).
- [9] D. Mattingly, *Living Rev. Rel.* **8**, 5 (2005).
- [10] V. A. Kostelecky and M. Mewes, *Phys. Rev. D* **69**, 016005 (2004).
- [11] V. A. Kostelecky and M. Mewes, *Phys. Rev. D* **70**, 031902 (2004).
- [12] V. A. Kostelecky and M. Mewes, *Phys. Rev. D* **70**, 076002 (2004).
- [13] L. B. Auerbach *et al.* [LSND Collaboration], *Phys. Rev. D* **72**, 076004 (2005).
- [14] P. Adamson *et al.* [MINOS Collaboration], *Phys. Rev. Lett.* **101**, 151601 (2008).
- [15] A. A. Aguilar-Arevalo *et al.* [MiniBooNE Collaboration], *Phys. Lett. B* **718**, 1303 (2013).
- [16] P. Adamson *et al.* [MINOS Collaboration], *Phys. Rev. D* **85**, 031101 (2012).
- [17] P. Adamson *et al.* [MINOS Collaboration], *Phys. Rev. Lett.* **105**, 151601 (2010).
- [18] B. Rebel and S. Mufson, *Astropart. Phys.* **48**, 78 (2013).
- [19] Y. Abe *et al.* [Double Chooz Collaboration], *Phys. Rev. D* **86**, 112009 (2012).
- [20] J. S. Diaz, T. Katori, J. Spitz and J. M. Conrad, *Phys. Lett. B* **727**, 412 (2013).
- [21] R. Abbasi *et al.* [IceCube Collaboration], *Phys. Rev. D* **82**, 112003 (2010).
- [22] K. Abe *et al.* [Super-Kamiokande Collaboration], *Phys. Rev. D* **91**, no. 5, 052003 (2015).
- [23] M. G. Aartsen *et al.* [IceCube Collaboration], *Phys. Rev. Lett.* **111**, 021103 (2013),
arXiv:1304.5356.

- [24] M. G. Aartsen *et al.* [IceCube Collaboration], *Science* **342**, 1242856 (2013), arXiv:1311.5238.
- [25] M. G. Aartsen *et al.* [IceCube Collaboration], *Phys. Rev. D* **89**, no. 6, 062007 (2014), arXiv:1311.7048.
- [26] M. G. Aartsen *et al.* [IceCube Collaboration], *Phys. Rev. Lett.* **113**, 101101 (2014), arXiv:1405.5303.
- [27] M. G. Aartsen *et al.* [IceCube Collaboration], *Phys. Rev. Lett.* **114**, no. 17, 171102 (2015), arXiv:1502.03376.
- [28] M. G. Aartsen *et al.* [IceCube Collaboration], *Astrophys. J.* **809**, no. 1, 98 (2015), arXiv:1507.03991 [astro-ph.HE].
- [29] O. Mena, S. Palomares-Ruiz and A. C. Vincent, *Phys. Rev. Lett.* **113**, 091103 (2014), arXiv:1404.0017.
- [30] S. Palomares-Ruiz, A. C. Vincent and O. Mena, *Phys. Rev. D* **91**, no. 10, 103008 (2015), arXiv:1502.02649.
- [31] W. Winter, *Phys. Rev. D* **90**, no. 10, 103003 (2014), arXiv:1407.7536.
- [32] K. Murase and S. Nagataki, *Phys. Rev. D* **73**, 063002 (2006).
- [33] P. Baerwald, S. Hummer and W. Winter, *Phys. Rev. D* **83**, 067303 (2011).
- [34] A. Palladino, G. Pagliaroli, F. L. Villante and F. Vissani, *Phys. Rev. Lett.* **114**, no. 17, 171101 (2015), arXiv:1502.02923
- [35] M. G. Aartsen *et al.* [IceCube Collaboration], arXiv:1412.5106 [astro-ph.HE].
- [36] M. G. Aartsen *et al.* [IceCube Collaboration], arXiv:1510.05228 [astro-ph.IM].
- [37] I. M. Shoemaker and K. Murase, *Phys. Rev. D* **93**, no. 8, 085004 (2016).
- [38] P. Lipari, M. Lusignoli and D. Meloni, *Phys. Rev. D* **75**, 123005 (2007).
- [39] T. Kashti and E. Waxman, *Phys. Rev. Lett.* **95**, 181101(2005), astro-ph/0507599.
- [40] M. Kachelriess, S. Ostapchenko and R. Tomas, *Phys. Rev. D* **77**, 023007 (2008), arXiv:0708.3047.
- [41] S. Hummer, M. Maltoni, W. Winter and C. Yaguna, *Astropart. Phys.* **34**, 205 (2010), arXiv:1007.0006.
- [42] C. A. Argelles, T. Katori and J. Salvado, *Phys. Rev. Lett.* **115**, 161303 (2015).
- [43] T. Katori, C. A. Argelles and J. Salvado, arXiv:1607.08448 [hep-ph].
- [44] G. Barenboim and C. Quigg, *Phys. Rev. D* **67**, 073024 (2003).
- [45] D. Hooper, D. Morgan and E. Winstanley, *Phys. Rev. D* **72**, 065009 (2005).

- [46] M. Bustamante, A. M. Gago and C. Pena-Garay, JHEP **1004**, 066 (2010).
- [47] M. C. Gonzalez-Garcia, M. Maltoni and T. Schwetz, Nucl. Phys. B **908**, 199 (2016)
doi:10.1016/j.nuclphysb.2016.02.033 [arXiv:1512.06856 [hep-ph]].
- [48] K. C. Lai, G. L. Lin and T. C. Liu, Phys. Rev. D **82**, 103003 (2010).